Journal of Catalysis **203,** 453–465 (2001)
doi:10.1006/jcat.2001.3324, available online at http://www.idealibrary.com on IDEAL®

Isomerization of *n*-Butane over Sulfated Al- and Ga-Promoted Zirconium Oxide Catalysts. Influence of Promoter and Preparation Method

J. A. Moreno and G. Poncelet[1]

Unité de Catalyse et Chimie des Matériaux Divisés, Université Catholique de Louvain, Place Croix du Sud, 2/17, B-1348 Louvain-la-Neuve, Belgium

Received April 6, 2001; revised June 8, 2001; accepted June 27, 2001

Isomerization of *n*-butane has been investigated at 250°C over sulfated zirconia, and Al- and Ga-promoted zirconias calcined at 650°C and activated at 450°C. The promoter (3 mol% as Al_2O_3 and Ga_2O_3) was introduced by both impregnation and coprecipitation, in order to examine the influence of the preparation method and the nature of the promoter on the catalytic properties. The catalysts were characterized by X-ray diffraction, Raman, and photoelectron spectroscopy (XPS). The total acidity was determined from ammonia-TPD measurements. The sulfate and OH stretching regions and the spectral modifications occurring upon ammonia adsorption were investigated by DRIFT spectroscopy. The nature of the acid sites prevailing at the activation and reaction temperature was clearly of Brønsted type, as observed by the IR characteristic NH_4^+ deformation band. With respect to sulfated zirconia, the promoted catalysts exhibited higher fractions of tetragonal structure, sulfate densities, and Brønsted acidity, all intervening in the catalyst efficiency and stability. Incorporation of the promoter via coprecipitation provided more efficient catalysts than via impregnation. Platinum addition improved the performances (conversion, long-term stability) of all catalysts, with this beneficial effect being relatively more spectacular for nonpromoted than for promoted sulfated zirconias. © 2001 Academic Press

Key Words: **butane isomerization; sulfated zirconia; Al-promoted sulfated zirconia; Ga-promoted sulfated zirconia.**

INTRODUCTION

Sulfated zirconia-based catalysts are considered as alternatives to the industrial platinum on chlorinated alumina catalysts for *n*-butane isomerization which require a continuous supply of a chlorine compound to maintain the activity (1). Arata (2) and Tanabe *et al.* (3) systematically studied sulfated zirconias. The low-temperature activity of these acid solids has been greatly improved by promotion with transition metals (e.g., Fe, Mn) but, as nonpromoted sulfated zirconias, these catalysts deactivate rapidly (4). In most cases, addition of the promoter was done by impregnation, before or after sulfating. Only in a limited number of studies, the second metal was introduced using a coprecipitation method. This is mainly because the role of the second metal has been considered as an additional phase providing new and different active sites (redox sites) and/or creating a synergistic effect with the acid sites of sulfated zirconia (5).

In recent years, sulfated zirconias promoted with aluminum have been reported in the literature. Sulfated ZrO_2–Al_2O_3 mixed oxides (with about 29 mol% Al_2O_3) and their platinum-impregnated forms were claimed as efficient catalysts for the skeletal isomerization of *n*-butane and other alkanes (6). A similar conclusion was formulated more recently for sulfated Al-promoted zirconium oxide microspheres prepared via a sol–gel method with Al_2O_3 contents in the 0.83–7.6 wt% range (7). Gao *et al.* (8) showed that the isomerization activity was optimal for a catalyst with 3 mol% Al_2O_3 prepared by a coprecipitation method. Supporting sulfated zirconias on γ-alumina (60 and 90 wt% SZ) increased the steady-state conversion by a factor of 2.5 compared with unsupported SZ, an improvement attributed to the enhanced content of strong Lewis acid sites (9, 10). The beneficial promoting effect of Al is not unanimous. For example, Angelescu *et al.* (11) obtained comparable conversions over sulfated Al-promoted zirconias (0.5 to 2.4 mol% Al_2O_3) and sulfated zirconia. Mesoporous sulfated zirconias and Al-doped forms exhibited similar activity in isobutane isomerization, aluminum contributing to the stability of the porosity by forming a surface coating (12).

In this study, *n*-butane isomerization has been investigated over sulfated, Al- and Ga-promoted zirconias and compared with sulfated zirconia. Two methods to introduce the promoter (3 mol% as M_2O_3) were compared: impregnation and coprecipitation. The aim was to investigate the eventual beneficial influence of these promoters in relation with the preparation method and nature of the promoter on the catalytic performances. The influence of platinum addition was also considered.

EXPERIMENTAL

Preparation Methods

Impregnation. An oven-dried (100°C, 24 h) commercial zirconium hydroxide (MEL Chemicals, XZO 631/01)

[1] To whom correspondence should be addressed. E-mail: poncelet@cata.ucl.ac.be.

was first impregnated with an aqueous solution containing the required amounts of $Al(NO_3)_3 \cdot 9H_2O$ (UCB) or $Ga(NO_3)_3 \cdot nH_2O$ (Johnson Matthey) in order to obtain solids with 3 nominal mol% Al_2O_3 or Ga_2O_3, calculated on the weight basis of ZrO_2. The slurries, in the proportion of 1 g of solid per milliliter of solution, were stirred for 1 h and dried at 100°C for 16 h. In a second step, the solids were impregnated with an adequate volume of 0.5 *M* sulfuric acid in order to have 10 wt% SO_4^{2-} based on the weight of ZrO_2. After drying at 100°C, the solids were calcined in static air for 3 h at 650°C, with temperature being linearly increased at a rate of 5°C min^{-1}. The sulfated aluminum- and gallium-impregnated catalysts are designated as SA*Z*i-3 and SG*Z*i-3, respectively, with A and G standing for Al and Ga, and *i* for impregnation method.

Coprecipitation. An ammonia solution (min 25%, UCB) was added dropwise under stirring (0.5 ml min^{-1}) to a 0.3 *M* solution of $ZrOCl_2 \cdot 8H_2O$ (Merck) wherein amounts of $Al(NO_3)_3 \cdot 9H_2O$ or $Ga(NO_3)_3 \cdot nH_2O$ corresponding to 3 mol% M_2O_3 (nominal) were previously dissolved, up to a final pH 8. Stirring was maintained for an additional 20 min. The precipitates were washed free of chlorides and dried overnight at 100°C. The mixed hydroxides were impregnated with 0.5 *M* sulfuric acid (10 wt% sulfate), dried for 16 h at 100°C, and calcined for 3 h at 650°C in static air (using the same ramp as above). The sulfated aluminum- and gallium-mixed oxides are denoted as SA*Z*c-3 and SG*Z*c-3, respectively, with *c* standing for coprecipitation method.

Pt-impregnated samples were prepared by adding the appropriate volume of a solution of platinum tetraammine chloride (Johnson Matthey) (1 mg of Pt per milliliter of solution) in order to deposit 0.3 wt% of Pt. Typically, 1 g of precalcined sulfated modified zirconia was mixed with 3 ml of the platinum salt solution, gently stirred, and evaporated overnight in an oven at 80°C.

Characterization

Chemical analyses of Al, Ga, and Zr were performed by inductively coupled plasma spectroscopy after a treatment of the samples with $NaOH–Na_2O_2$ and dissolution in hydrofluoric acid. The sulfate content was determined with a HF-400 LECO analyzer. The BET specific surface areas were obtained from nitrogen adsorption–desorption isotherms established at 77 K with an ASAP 2000 sorptometer (Micromeritics) on samples previously outgassed *in situ* for 6 h at 200°C. Thermogravimetric analyses between room temperature and 1000°C (ramp of 10°C min^{-1}) were carried out over 10-mg samples with TGA/SDTA 851 equipment (Mettler-Toledo), under air flow of 100 ml min^{-1}.

The total acid content was established by temperature-programmed desorption of ammonia (NH_3-TPD) (ramp of 10°C min^{-1}). The samples (0.2 g), previously activated *in situ* at 500°C for 30 min and cooled at 100°C in flowing He (65 ml min^{-1}), were saturated with successive pulses of ammonia. After a purge with helium for 1 h at 100°C, the ammonia evolved during TPD between 100 and 500°C (ramp of 10°C min^{-1}; helium flow of 65 ml min^{-1}) followed by a plateau for 30 min was collected by bubbling the effluent at the exit of the TC detector in 0.2 *M* boric acid solution. The amount of ammonia released was determined by back-titration of the solution with 0.005 *M* sulfuric acid, using a Digital II burette (precision ±0.01 ml, Brand) and mixed indicator 5 (Merck).

X-ray diffraction (XRD) patterns of the calcined samples were recorded in the 5–65° 2θ range at a scanning rate of 0.03° 2θ every 5 s with a Kristalloflex D-5000 (Siemens) apparatus (monochromated Cu$K\alpha$ radiation). The volume fraction of the monoclinic phase was evaluated by following the method of Toraya *et al.* (13). Because of partial peak overlapping, decomposition was performed with Diffract-AT software, peak simulation being done with a Lorentz function and successive iterations until the width of the different peaks did not differ by more than 5%.

Raman spectra were recorded under ambient conditions with a Labram II spectrometer (Dilor-Jobin Yvon-Spex) equipped with a He–Ne laser (λ, 632.8 nm; 25 mW; slit width, 200 μm; resolution, 3 cm^{-1}) after three scans with accumulation time of 60 s each.

XPS spectra were obtained with an SSI X probe spectrometer (SSX-100/206, Surface Science Instruments) equipped with a monochromatized microfocused Al$K\alpha$ source. The operating conditions have been indicated elsewhere (14). The binding energies of the O 1*s*, Al 2*s*, Ga 3*p*, Zr 3*d*, and S 2*p* peaks were referenced to that of the *C*–(C,H) component of the C 1*s* peak of adventitious carbon at 284.8 eV. Peak decomposition was performed with a least-squares fitting routine, using a Gauss/Lorentz ratio of 85/15 and after nonlinear baseline subtraction. The atomic concentration ratios were calculated from the peak areas normalized on the basis of acquisition parameters and sensitivity factors provided by the manufacturer.

Diffuse reflectance Fourier transform infrared (DRIFT) spectra were obtained with an IFS55 Equinox spectrometer (Bruker) equipped with an MCT detector and an environmental temperature-controlled chamber (Spectra-Tech). Spectra (200 scans with a resolution of 4 cm^{-1}) were recorded in flowing dry air (50 ml min^{-1}) at room temperature and after successive heating to 450°C (activation temperature), and cooling to 250°C (reaction temperature). The air flow was passed through a water trap (Gas purifier, Alltech) prior to its admission into the analysis cell. At this temperature, the cell was purged with helium for 20 min and a flow of diluted ammonia (0.5 vol% in He; 50 ml min^{-1}) was passed for 20 min, followed by an additional purge with pure helium for another 20 min. Spectra were recorded between 250 and 450°C at temperature intervals of 50°C and under flowing helium.

Isomerization of *n*-butane was carried out in a continuous-flow microreactor (8 mm i.d.) operated at atmospheric pressure. The catalyst (0.5 g, 0.2–0.315 mm fraction) was introduced in the reactor between quartz wool plugs, and activated in flowing dry air (50 ml min^{-1}, Air Liquide) at 450°C for 1.5 h. Cooling at the reaction temperature (250°C) was done in flowing air. For the Pt-impregnated catalysts, the air activation was followed, after a helium purge, by a reduction in flowing hydrogen (50 ml min^{-1}) for 1.5 h at 250°C prior to the admission of the reaction mixture. The feed consisted of a mixture of 1 ml min^{-1} of *n*-butane (Air Liquide, 99.95%) and 10 ml min^{-1} of H_2 (Air Liquide, 99.90%). The WHSV was 0.3 g of butane per gram catalyst per hour. The gases were passed through "Hydro-purge" and "Oxy-trap" (Alltech Associates) in order to remove water and traces of oxygen. It was verified that under these conditions diffusion limitations were absent. The reaction products were analyzed on-line in a gas chromatograph (Hewlett-Packard 5880A) equipped with a TC detector and a 50-m-long Al_2O_3/KCl capillary column to separate the products. Conversion, yields, and selectivity were calculated on a carbon number basis.

RESULTS

Catalysts Characterization

Characterization results of the nonpromoted sulfated zirconia and the promoted catalysts obtained by impregnation and coprecipitation are given in Table 1. The catalysts prepared by impregnation developed larger surface areas. All catalysts exhibited type II isotherms indicative of the presence of macropores with, for SZ and the co-precipitated catalysts, H2–H3 hysteresis loops suggesting nonuniform slit-shaped mesopores (15). The total pore volumes of the SMZ*i*-3 catalysts (M = Al, Ga) were about twice as high as for the SMZ*c*-3 catalysts, with intermediate value for nonpromoted SZ. Negligible micropores were present (0.005 $cm^3\ g^{-1}$ for the SMZ*i* catalysts, 0.001–0.002 $cm^3\ g^{-1}$ for the other ones). All the samples showed unimodal BJH pore size distribution with pore diameter in the 2.6–3.4 nm range.

The sulfate contents of the samples (Table 1) decreased in the order SAZ > SGZ > SZ, with small differences between the impregnated and coprecipitated samples. Since they all were impregnated with similar amounts of

TABLE 1

Characterization Data of the Different Catalysts

	Sample				
	SZ	SAZi-3	SGZ*i*-3	SAZ*c*-3	SGZ*c*-3
Textural properties					
S_{BET} ($m^2\ g^{-1}$)	96	137	125	103	97
V_p ($cm^3\ g^{-1}$)	0.105	0.146	0.137	0.076	0.083
Sulfate content (wt%)					
c.a.	4.86	8.14	7.26	8.15	6.50
TGA	4.34	7.65	6.87	7.15	5.82
Sulfate density					
(SO_4^{2-} nm^{-2})	3.2	3.7	3.6	5.0	4.2
Surface coverage (%)	79.3	93.1	91.0	124.0	105.0
Water content (wt%)					
TGA	3.12	5.97	5.03	5.25	3.93
Monoclinic fraction (%)[a]	40.6	12.8	14.3	5.4	<5
XPS analysis					
S/Zr					
c.a.	—	0.126	0.118	0.119	0.095
xps	0.136	0.147	0.152	0.198	0.160
M/Zr					
c.a.	—	0.058	0.060	0.055	0.056
xps	—	0.048	0.035	0.061	0.045
Acidity					
NH_3-TPD (μmol g^{-1})	248	342	394	298	284
μmol m^{-2}	2.58	2.50	3.15	2.89	2.93
μmol SO_4^{2-}/μmol NH_3	1.98	2.33	1.82	2.70	2.29
NH_4^+-IR (a.u. m^{-2})					
250°C	1.42	2.41	2.45	2.14	2.44
450°C	0.003	0.168	0.256	0.194	0.227

[a] Method of Toraya *et al.* (13); c.a., chemical analysis.

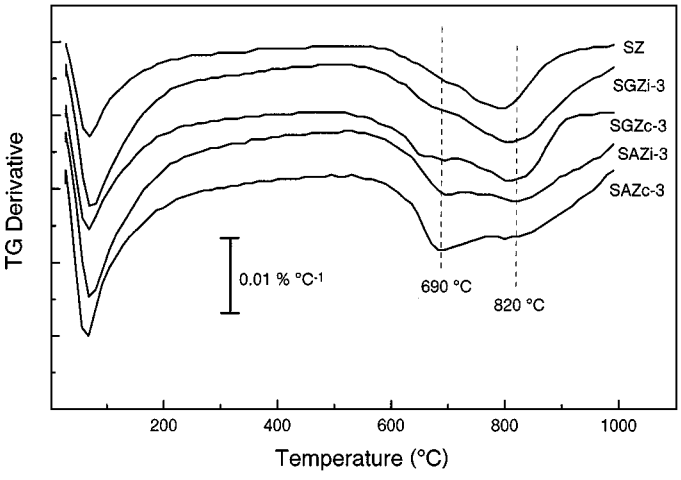

FIG. 1. DTG curves of the different catalysts previously calcined at 650°C and stored under ambient conditions.

sulfate and calcined at 650°C, this sequence suggests that, independent of the preparation method, promotion with Al and Ga had a favorable effect on sulfate retention with respect to nonpromoted sulfated zirconia. In terms of surface coverage by sulfate, this table also shows that, assuming a surface area of 0.25 nm^2 for a sulfate group (16), the amounts of sulfate corresponded to less than the theoretical monolayer capacity for the solids obtained by the impregnation method, whereas monolayer coverage was achieved for the coprecipitated samples, with an excess for SAZ*c*-3.

The DTG curves of the different catalysts (Fig. 1) showed a first weight loss with a minimum below 100°C due to the removal of water. The losses above 500°C are associated with the decomposition of the sulfate. The existence of two minima (near 690 and 820°C) suggests sulfate species with distinct thermal stability, possibly reflecting different sulfate–oxide interactions. The first component was relatively more developed than the second one for the SAZ catalysts compared with SGZ. Sulfated zirconia showed a small contribution at 680°C and a main minimum at 790°C, namely, about 30°C lower than for the promoted catalysts. Such a temperature difference has been attributed to the stabilizing effect of the Al promoter on the sulfate species (17). The sulfate contents determined from the weight losses between 500 and 1000°C are compared in Table 1 with those obtained by chemical analysis. Both sets of values followed a similar sequence, with a linear relationship between them. The higher values determined by chemical analysis are probably due to the different temperatures used for the determination of sulfate (1500°C vs 1000°C for the TGA). This table also shows that the percentages of water taken up by the samples previously calcined at 650°C and kept under ambient conditions were proportional to the sulfate content.

The XRD patterns of the catalysts (Fig. 2) mainly showed the reflections of tetragonal ZrO_2 which were noticeably more intense for the coprecipitated than for the impregnated samples. Sulfated zirconia contained an appreciable amount of the monoclinic phase. As seen in Table 1, the volume fraction of the monoclinic phase was about 3 times higher in SZ than in SAZ*i*-3 and SGZ*i*-3, and 6–8 times more than in SAZ*c*-3. No reliable figure could be obtained for SGZ*c*-3 because of the very weak peak intensity, but the monoclinic fraction was well below 5%.

The Raman spectra (Fig. 3) exhibited the characteristic bands of the tetragonal phase at 643, 458, 318, 278, and 150 cm^{-1} (18). SZ, SAZ*i*-3, and SGZ*i*-3 showed additional bands at 180, 189, 220, 330–340, 383, 475, 505(sh), 535, 555, and 615 cm^{-1}, typical of the monoclinic structure (see reference spectrum of ZrO_2 calcined at 650°C). The doublet at 180–189 cm^{-1} was barely observed for the coprecipitated samples. It is interesting to mention that the spectra of the coprecipitated oxides (no sulfate) and their sulfated forms were much similar (spectra not shown here). The promoted samples exhibited Raman bands due to S–O stretching vibrations at 983, 1008, and 1029 cm^{-1}. The band at 983 cm^{-1}, absent in SZ, could be related with sulfate interacting with Al and Ga. A band at 982 cm^{-1} was, indeed, observed for a sulfated γ-alumina calcined at 600°C. This band was more intense for the Al-promoted samples relative to the Ga-promoted ones, which could be related to the sulfate contents. In the literature, a doublet at 1000–1030 cm^{-1} has been attributed to two sulfate species with slightly different distortions (19). Of course, under the conditions adopted (rehydrated samples, atmospheric

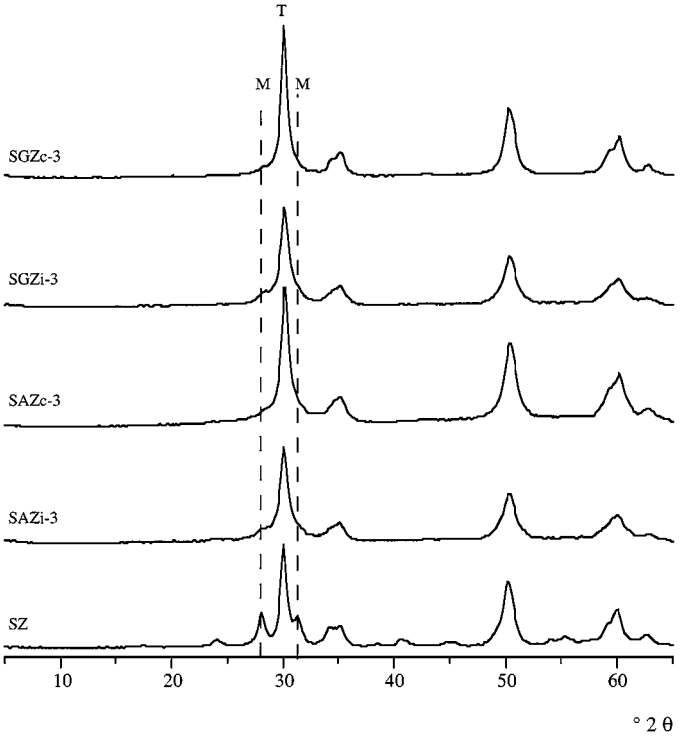

FIG. 2. XRD patterns of the series of catalysts calcined at 650°C.

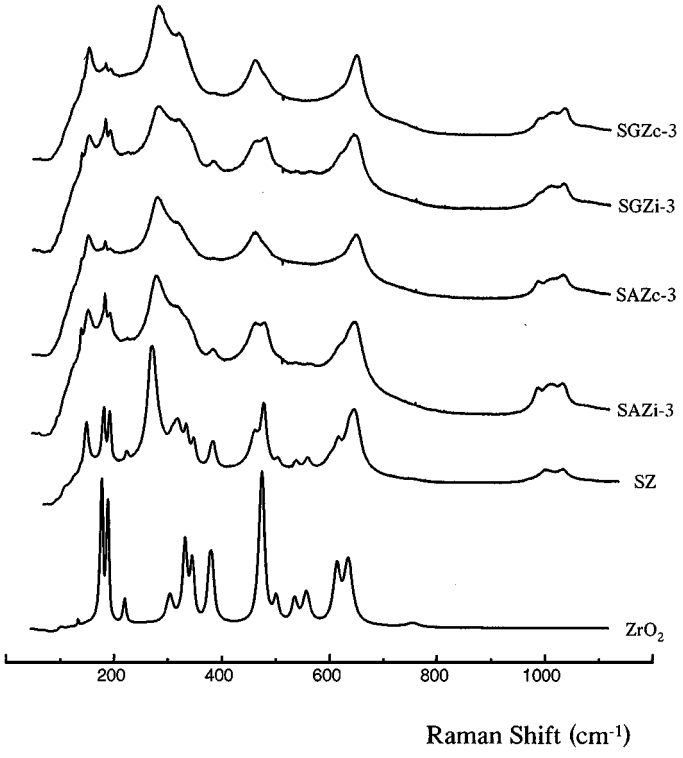

FIG. 3. Raman spectra recorded at room temperature.

conditions, room temperature), the S=O stretching mode (around 1400 cm^{-1}) observed in *in situ* recordings (high temperature, vacuum) (19) was absent.

Analysis of the XPS spectra showed for all catalysts two components for the O 1*s* peak, with BE values of 530.5 and 532.4 eV. The binding energy of the O 1*s* of the Zr–O component and Zr 3*d*(5/2 and 3/2) peaks was 0.6 eV higher relative to ZrO_2 (with BE of O $1s = 529.9$ eV). The O 1*s* peak of the S–O bond had a binding energy of 532.4 eV (532.6 eV in $Zr(SO_4)_2$). This 0.6 eV shift reflects an electron-withdrawing effect by the sulfate groups at the surface of zirconium oxide. In stoichiometric zirconium sulfate, the BE of the Zr 3*d* peaks was 2.3 eV higher than in ZrO_2. The BE values of the Ga 3*p*(3/2 and 1/2) levels in SGZ*c*-3 were 105.9 and 109.5 eV, respectively, which is 0.3 eV higher than in Ga_2O_3. For SGZ*i*-3, the binding energies were similar to those found in gallium oxide (105.6 and 109.2 eV). For the Al-promoted catalysts, the BE of the Al 2*s* peak was slightly higher (0.2–0.3 eV) than in Al_2O_3 (precision limit: 0.1–0.2 eV). The S 2*p*(3/2 and 1/2) peaks of the promoted and non-promoted SZ had similar binding energies. All the samples exhibited, as expected, higher surface than bulk S/Zr atomic ratios (Table 1). The lower M/Zr atomic ratios of the catalysts prepared by impregnation relative to those obtained by coprecipitation may be accounted for by a dilution effect due to the higher surface areas of the former ones. For the same reason, the former catalysts also had a lower S/Zr ratio with respect to the SAZ*c*-3 and SGZ*c*-3 catalysts.

The quantities of ammonia released in TPD measurements are given in Table 1 (acidity). Higher amounts were found for the promoted catalysts than for sulfated zirconia. The catalysts prepared by the impregnation method adsorbed more ammonia than those obtained by coprecipitation, the differences decreasing when normalizing to the surface areas, with slightly higher values for SGZ*c*-3 than SAZ*c*-3. The sulfate/acid ratios (expressed as micromoles of SO_4^{2-} per micromole of NH_3) were between 1.8 and 2.7 (with the higher ratio for SAZ*c*-3 with overlayer sulfate), indicating that each sulfate group did not generate an adsorption site. The results obtained with this method should be interpreted with caution since they represent global ammonia uptakes which do not differentiate physisorbed ammonia (which cannot be excluded at 100°C) from that in interaction with Lewis and Brønsted acid sites, as well as ammonia possibly interacting with NH_4^+ (20). Besides, the validity of the NH_3-TPD method for the determination of the Brønsted acidity, at least in the case of microporous solids (zeolites), has been recently questioned (21). However, as will be discussed in the next section, both Brønsted and Lewis acidities were clearly identified by DRIFT spectroscopy of adsorbed ammonia.

DRIFT Spectroscopy before and after Ammonia Adsorption

DRIFT spectra were recorded under conditions reproducing as closely as possible those of the activation treatment (450°C) and reaction temperature (250°C), and in particular the hydration state which has a critical importance on the catalyst acidity and activity (5). As shown in Fig. 4a, similar spectra were obtained in the sulfate region (1000–1400 cm^{-1}) after activation in air at 450°C, with a band at 1394–1397 cm^{-1}, more intense for the promoted catalysts obtained by impregnation, and poorly resolved ones near 1310, 1200–1220, and a broad absorption with components near 1010 and 1025–1035 cm^{-1}. The small band at 1620 cm^{-1} indicated the persistence of some residual water. The band around 1220 cm^{-1} was a little more intense for the Al-promoted catalysts, possibly in relation with the species with DTG minimum at 690°C. In sulfated zirconia, bands at 1390–1394 cm^{-1}, 1200–1220 cm^{-1}, and 1025–1035 cm^{-1} have been attributed to the $\nu_{S=O}$ of surface $(ZrO)_3S{=}O$ species and/or to the asymmetric O=S=O stretching mode of $(Zr)_2SO_2$ species, the symmetric O=S=O stretching mode of $(Zr)_2SO_2$ species, and the ν_{S-O} stretching mode(s) of all surface sulfates, respectively (22, 23). Bands between 1000 and 1035 cm^{-1} would indicate more complex structures, possibly at different crystallographic surfaces (24), or sulfate species with slightly distorted configurations (19) (see Raman results).

The OH stretching region (Fig. 4b) showed a main band at 3625–3630 cm^{-1} and a shoulder at 3720 cm^{-1}. Another band at 3560 cm^{-1}, better resolved at intermediate temperatures

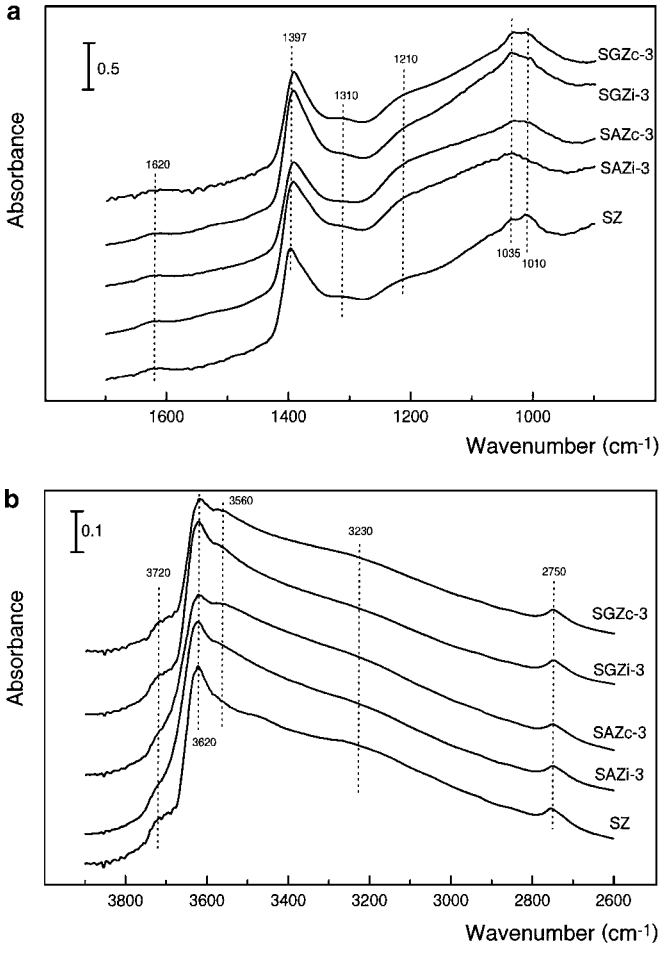

FIG. 4. (a) DRIFT spectra at 450°C of the sulfate stretching region. (b) DRIFT spectra at 450°C of the OH stretching region.

(higher hydration level) than at 450°C, was more intense for the coprecipitated than the impregnated catalysts, and nearly absent for nonpromoted SZ. A broad weak band centered around 3230 cm^{-1} was also noticed. Bands at 3720 and 3620 cm^{-1} have been assigned to isolated and bridging OH groups coordinated to more than one Zr cation, respectively, whereas a band at 3560 cm^{-1} would be due to nonspecified hydroxyl groups present in sulfated zirconia (absent in pure zirconia) (25). A broad band at 3250–2950 cm^{-1} has been attributed to terminal ZrOH groups where the protons are substituted by HSO_4^- anions creating a new type of Brønsted sites, presumably protons forming multicenter bonds with sulfate anions (26), or to OH groups strongly interacting with each other or with the surface through hydrogen bonding (27). The band at 2750 cm^{-1} could be assigned to an overtone of the band near 1390 cm^{-1} (26).

Subsequent cooling at 250°C (reaction temperature) did not significantly modify the spectra in the S=O and S–O stretching regions. A limited rehydration apparently occurred as inferred from the increased intensity of the band at 1615–1620 cm^{-1} which, in more hydrated samples, was located at 1635 cm^{-1}. Also, the band at 1310 cm^{-1} slightly increased. In the OH stretching region, the intensity of the bands at 3560 and near 3230 cm^{-1} increased relative to that at 3630 cm^{-1}. These modifications resemble those observed by Gonzalez *et al.* (28) upon addition of controlled amounts of water to a dehydrated sulfated zirconia. These authors attributed a band around 1600 cm^{-1} to an overtone of an OH bending mode at 800 cm^{-1} probably associated with the hydroxyl stretching at 3640 cm^{-1}, pointing to the dissociative adsorption of water. Morterra *et al.* (29) questioned this attribution and rather assigned a band at 1600–1610 cm^{-1} and three OH stretching modes at 3590, 3250, and 3170 cm^{-1} to H_3O^+ groups free from the diffuse H-bondings supposed typical of more hydrated stages, and having localized interaction with anionic groups (30). These authors related the occurrence of this species with the development of sulfate species having a slightly more ionic character (bands at 1300 and 1130 cm^{-1}). This attribution appears consistent with the spectral features mentioned above and could account for the small increase of intensity of the band at 1310 cm^{-1} in the samples cooled at 250°C, the one at 1130 cm^{-1} being probably hidden in the broad envelope above 1200–1220 cm^{-1}.

Ammonia was adsorbed on the samples cooled at 250°C, and the spectra were recorded after a helium purge for 20 min at that temperature, and after successive heating to 450°C under flowing helium. All the spectra (including those of SZ) exhibited features qualitatively similar to those illustrated in Figs. 5a and 5b for SA*Zc*-3. It was verified that longer exposure times to ammonia did not modify the spectra. As shown in Fig. 5a, adsorption of ammonia brought about a significant decrease of intensity of the band at 1394 cm^{-1} with a shift to 1355 cm^{-1}, the development of a new band centered at 1290–1295 cm^{-1}, and an upward shift of the components at 1035 and 1015 cm^{-1} to 1065–1055 cm^{-1}. An intense band appeared near 1430 cm^{-1}, assigned to the asymmetric deformation of NH_4^+ (proton transfer from OH to NH_3), and a tiny one at 1609 cm^{-1}, less intense than that near 1615–1620 cm^{-1} before ammonia adsorption, probably the asymmetrical deformation of NH_3 adsorbed on Lewis sites, and apparently indicating the displacement of water molecules by ammonia. A similar effect was observed by Morterra *et al.* (30) upon pyridine adsorption on sulfated zirconia. The small intensity of this band points to a low content of Lewis sites. Table 2 gives the position of the S=O band before and after adsorption of ammonia for the different catalysts. Larger shifts ($\Delta\nu_{S=O}$) were observed for the promoted catalysts compared with SZ. In the high-frequency region (Fig. 5b), ammonia adsorption caused the disappearance of the OH band near 3720 cm^{-1}. The band at 3634 cm^{-1} slightly decreased, and the band at 3570 cm^{-1} broadened and shifted at 3550 cm^{-1}. Several N–H stretching bands were noticed at 3360, 3270, 3173, 3046, and 2828 cm^{-1}. The position of these bands is similar to that observed by Teunissen *et al.* (31) for doubly

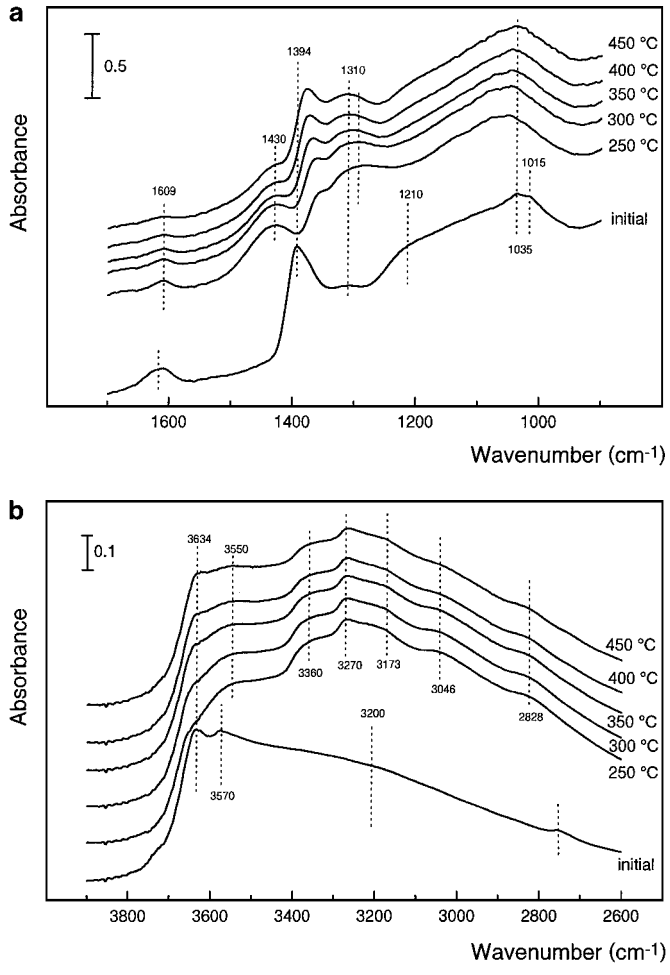

FIG. 5. (a) DRIFT spectra in the sulfate region of SA*Zc*-3 recorded at 250°C before and after ammonia adsorption, and after successive heating at increasing temperatures in flowing helium. (b) Same as Fig. 5a in the OH and NH stretching region.

(3040 and 2800 cm^{-1}) and triply bonded NH_4^+ (3360 and 3270 cm^{-1}) in mordenites. However, when ammonia is adsorbed on ZrO_2, only two bands are observed at 3380 and 3280 cm^{-1} which have been assigned to the asymmetric and symmetric N–H stretching vibrations of ammonia coordinated to Lewis sites (32). In this study, bands at 3350 and 3256 cm^{-1} (and at 1610 cm^{-1}) were as well observed upon ammonia adsorption on pure ZrO_2, therefore supporting the latter assignment for the N–H bands at 3360 and 3270 cm^{-1}. Based also on the analogy with reported values (33), the bands at 3046 and 2828 cm^{-1} can be attributed to N–H stretching of NH_4^+. The assignment of the band at 3173 cm^{-1} is not clear: N–H of coordinated NH_3 by Topsoe *et al.* (33); overtone of the δ_{as} of NH_3-L at 1605 cm^{-1} by Ramis *et al.* (34). Zecchina *et al.* (35) assigned bands at 3115 and 2865 cm^{-1} of ammonia adsorbed on zeolites to overtones of N–H doublets at 1450–1400 cm^{-1} (of NH_4^+) and their combination with bending modes at around 1650 cm^{-1}. The absence of fine structure of the absorption centered near 1430 cm^{-1} (Fig. 5a) makes it impossible to detect possible bi- and tridentate NH_4^+ species with different symmetries, as clearly observed in the case of zeolites. Of course, the rather different nature of both types of solids and, in particular, the essentially microporous structure of zeolites and the nature of the Brønsted acid sites (bridging $Si–OH–Al^{IV}$) have to be taken in account.

Successive heating to 450°C (Fig. 5a) brought about a progressive diminution of the NH_4^+ (1430 cm^{-1}) and NH_3–L (1609 cm^{-1}) bands, an upward shift of the S=O band to higher wavenumbers, a decrease of the broad band near 1295 cm^{-1} with an upward shift to 1310–1315 cm^{-1}, and a downward shift of the band at 1051 cm^{-1} ($\nu_{S–O}$) to 1034 cm^{-1}. For none of the promoted samples was the initial spectrum completely restored after heating at 450°C. For SZ, the ammonium band at 1430 cm^{-1} was nearly totally eliminated at 450°C, with the one at 1609 cm^{-1} (NH_3–L) relatively less affected. The intensity of the band at 1310–1315 cm^{-1} was significantly reduced and, as shown in Table 2, the $\nu_{S=O}$ band was back at 1386 cm^{-1}, namely, 7 cm^{-1} lower than its initial position (1393 cm^{-1}), and its initial intensity was almost restored. For the Al- and Ga-promoted samples, the ammonium band (1430 cm^{-1}) after heating at 450°C remained more intense than in SZ, with the S=O band being shifted back to 1380 cm^{-1} for the Al samples, and to 1377 cm^{-1} for the Ga samples, namely, a difference of 11–17 cm^{-1} with respect to the initial positions. As for SZ, the band at 1609 cm^{-1} was still visible. Also, the band around 1300 cm^{-1} remained more intense compared to that of SZ. In the high-frequency region (Fig. 5b), the initial structure of the OH bands was not recovered after heating at 450°C, and all the N–H stretching bands were still visible. The incomplete removal of ammonia associated with the position of the S=O stretching band at lower wavenumbers than before ammonia adsorption (Table 2), and the persistence of the different N–H bands between 3400 and 2800 cm^{-1} suggests strong Lewis and Brønsted acid sites, with the latter ones being probably stronger for the promoted catalysts relative to nonpromoted sulfated zirconia, as also suggested by the data of Table 2 (differences of the S=O band position before and after ammonia adsorption, and after desorption at 450°C).

TABLE 2

Band Position of the $\nu_{S=O}$ Mode (cm^{-1}) before and after Adsorption of Ammonia at 250°C, and after Desorption at 450°C

Catalyst	$\nu_{S=O}$ Before	$\nu_{S=O}$ After	$\Delta\nu_{S=O}$	$\nu_{S=O}$ after desorption at 450°C
SZ	1393	1363	30	1386
SA*Zi*-3	1392	1355	37	1380
SG*Zi*-3	1393	1358	35	1378
SA*Zc*-3	1392	1355	37	1381
SG*Zc*-3	1394	1355	39	1377

These observations are consistent with literature data. Gonzalez *et al.* (28) observed a band at 1430 cm^{-1}, the intensity of which increased upon incremental coverage of sulfated zirconia by ammonia. A tiny band at 1600–1606 cm^{-1}, whose intensity was barely affected by increasing amounts of ammonia adsorbed, was tentatively assigned to coordinatively bound NH_3, thus pointing to a small number of L sites. In parallel, the intensity of the band at 1420–1370 cm^{-1} decreased and that of a new band 1280 cm^{-1} increased. Morterra *et al.* (30) attributed the decrease of the separation between the two uncoupled S–O vibrations (in this study, $\Delta\nu = 365$ cm^{-1} (1395–1030 cm^{-1}) before NH_3 adsorption, and $\Delta\nu = 300$ cm^{-1} (1355–1055 cm^{-1}, after adsorption) as a decrease of the highly covalent character of the S=O bond to a lesser covalent bond. The appearance of a band at 1295 cm^{-1} is interpreted as a change of sulfate species with covalent character to sulfate with ionic character. The weakly intense band at 1310 cm^{-1} before ammonia adsorption could be assigned to such species. However, the band at 1295 cm^{-1} should also contain the δ_{sym} mode of NH_3–L. Perhaps the shift of the band at 1295 cm^{-1} to 1315 cm^{-1} upon heating observed in this study would indicate a distribution of Lewis sites with different strengths (32, 36). Tanabe *et al.* (3) considered the ability of the sulfate species to accommodate electrons from an adsorbed basic molecule as the driving force to generate highly acidic properties.

The integrated areas of the ammonium band at 250°C and after heating at 450°C, normalized to the sample surface area exposed to ammonia (in arbitrary units per square meter), are compiled in Table 1 (acidity, NH_4^+-IR). The value obtained at 250°C for SZ was markedly smaller than for the promoted catalysts. Those of the Ga-promoted samples were superior to the Al-promoted ones, with a significantly lower value for SAZ*c*-3 (consistently with the NH_3-TPD data). This latter sample had overlayer sulfates, suggesting adsorption sites partly inaccessible to ammonia or less sites. After heating at 450°C, there was an approximate 10- to 14-fold decrease of the acid densities for the promoted catalysts, and a factor of over 400 for SZ. These data indicate that promotion with Al and Ga brought about an important increase of the strong Brønsted acidity with respect to nonpromoted sulfated zirconia. In addition, the smaller temperature effect on the removal of ammonia for the promoted catalysts suggests B sites with higher strength than in sulfated zirconia.

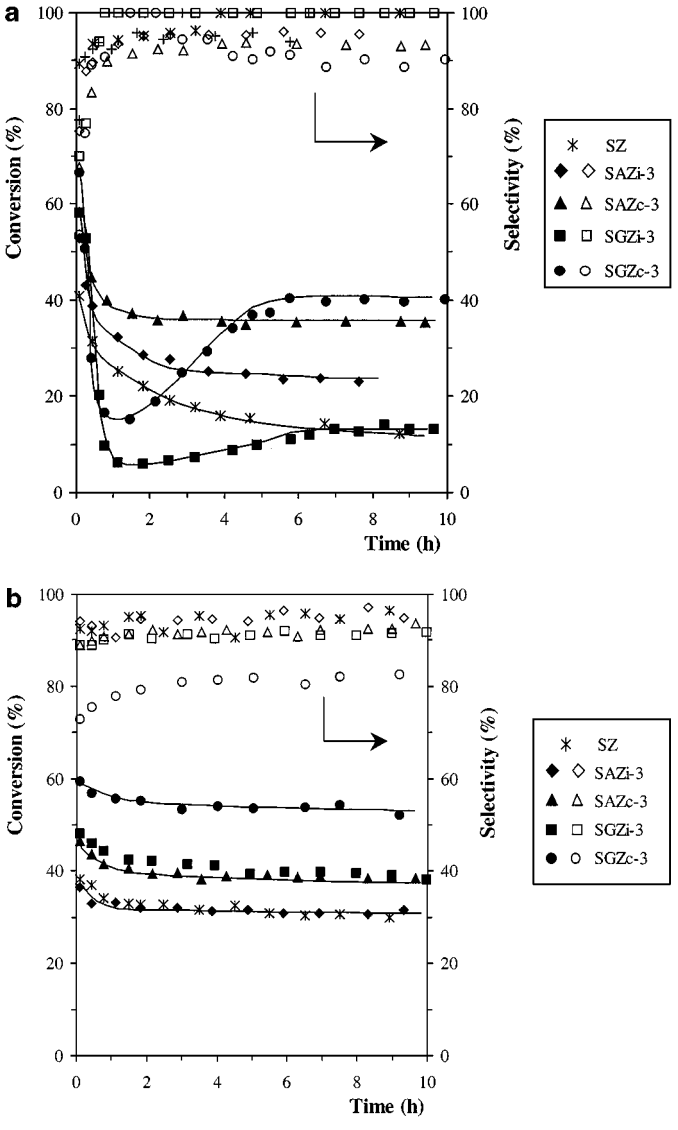

FIG. 6. (a) Conversion–time curves for the different catalysts. (b) Conversion–time curves for the Pt-impregnated catalysts.

Catalysis

The conversion–time curves obtained at 250°C over the nonpromoted and promoted catalysts are compared in Fig. 6a. All the promoted catalysts exhibited higher initial conversions than SZ. For the Ga-promoted catalysts, a dramatic loss of conversion occurred within the first hour of reaction so that they became markedly less active even than SZ. Beyond 1 h, the conversion started to increase again. For SGZ*c*-3, the conversion equalized that of SZ after about 2 h of reaction; after about 5–6 h, it was the most active catalyst. For SGZ*i*-3, it took about 7 h to reach the same conversion level as SZ. At steady conversion, the catalysts prepared by coprecipitation were more efficient than those obtained by impregnation. In addition, promotion also had a positive effect on the long-term stability of the catalysts. At steady conversion, the selectivities to i-C4 were in the range 90–96% for the more active catalysts, and 100% for the less active SZ and SGZ*i*-3 catalysts.

In order to find an explanation for the unexpected catalytic behavior of the Ga-promoted catalysts, XRD patterns of separate samples of SGZ*c*-3 having reacted for 1 h (minimum conversion) and 15 h (steady conversion) were recorded. No difference with respect to the fresh catalyst was observed, therefore excluding detectable phase

modification. XPS analysis of these samples (using a ceramic sample holder to avoid charging effects) showed some changes of the surface atomic compositions, with higher S/Zr and Ga/Zr ratios for the sample examined after 1 h of reaction (0.146 and 0.049, respectively, vs 0.143 and 0.039 for the fresh catalyst, and 0.142 and 0.046 after 15 h reaction). DRIFT spectra recorded at 250 and 450°C of the sample having reacted for 1 h showed a marked asymmetry of the band at 1394 cm^{-1}, with a component at about 1370 cm^{-1}. A less marked asymmetry was also observed for the sample after 15 h reaction. This contrasts with the fresh catalyst, which exhibited a symmetrical band at 1394 cm^{-1}. Bands at 1394 and 1370 cm^{-1} have been attributed to S=O stretching of $(ZrO)_3S{=}O$ species on a different crystal faces (22, 37, 38). It has been shown that a sulfated Fe-promoted zirconia with 2.5 wt% sulfate exhibiting only a band at 1370 cm^{-1} (at 450°C) was totally inactive in *n*-butane isomerization compared with catalysts with higher sulfate content exhibiting a single $\nu_{S=O}$ band at 1394 cm^{-1} (14). These observations suggest partial migration of less tightly bonded sulfate species to another face of the crystals and, possibly, a redistribution in the course of the reaction. However, it could well be that this effect merely constitutes a consequence rather than the origin of the observed phenomenon. Work in progress, indeed, indicates that the particular behavior of SGZ*c* catalysts is not always observed and depends on several factors such as calcination and activation temperature, nature of the sulfate source, amount of sulfate, platinum addition (as shown below), and space velocity. Therefore, a definitive explanation is premature. *In situ* spectroscopic investigation during reaction could cast more light on the unusual behavior of these catalysts.

Figure 6b shows the conversion vs time curves obtained over the series of Pt-impregnated catalysts. All the catalysts, including sulfated zirconia, exhibited higher steady conversions compared with the Pt-free forms. The fast decrease of conversion during the first hour of reaction observed in Fig. 6a was nearly absent, with the steady regime being readily attained. The presence of platinum also totally suppressed the atypical behavior of the Ga-promoted catalysts. At steady conversion, Pt/SGZ*i*-3 was this time more active than Pt/SAZ*i*-3 (reproducibility 3–5%), and the conversion of Pt/SZ was improved by a factor of about 2.6 with respect to SZ, with a conversion–time curve similar to that of Pt/SAZ*i*-3.

The conversions, selectivities to i-C4, and yields of the reaction products after 5 min and at steady regime, without and with platinum, are compared in Tables 3a and 3b, respectively. Without Pt (Table 3a), besides i-C4 as the main product, only propane was formed during the first part of the reaction over SZ (up to about 4 h). Over the promoted catalysts, propane was produced throughout, together with some C2 and i-C5 (only in the first 30–40 min). For all the Pt-impregnated catalysts (Table 3b), the conversions at 5 min were lower than those over the Pt-free forms, with this decrease being relatively more important for the promoted catalysts, whereas the steady conversions were significantly enhanced, with a substantially higher relative gain for Pt/SGZ than for Pt/SAZ catalysts. The more active catalysts were slightly less selective to i-C4, owing to enhanced side products (hydrogenolysis/cracking). Over the promoted catalysts, ethane and propane appeared throughout the reaction with, for Pt/SGZ*c*-3, also some methane. No i-C5 was found among the reaction products over the Pt-loaded catalysts. In no case (without or with Pt) were olefins formed, even in amounts below the integration limit.

TABLE 3

Conversion, Selectivity and Yields after 5 min Reaction and at Steady Regime over Pt-Free and Pt-Impregnated Catalysts

Catalyst	Conv. (%)	Select. (%)	Yield (%) C_1	C_2	C_3	i-C_4	i-C_5
(a) Pt-Free Catalysts							
After 5 min							
SZ	40.9	89.4	0.0	0.0	4.3	36.6	0.0
SAZ*i*-3	53.0	75.3	0.0	0.6	9.8	39.9	2.7
SGZ*i*-3	58.3	69.9	0.0	1.0	13.4	40.8	3.2
SAZ*c*-3	58.2	67.7	0.0	0.9	15.1	39.4	2.8
SGZ*c*-3	66.6	53.5	0.0	2.4	25.3	35.6	3.3
Steady regime							
SZ	11.5	100	0.0	0.0	0.0	11.5	0.0
SAZ*i*-3	23.5	95.8	0.0	0.0	1.0	22.5	0.0
SGZ*i*-3	14.3	100	0.0	0.0	0.0	14.3	0.0
SAZ*c*-3	35.5	93.3	0.0	0.0	2.4	33.1	0.0
SGZ*c*-3	40.3	90.4	0.0	0.4	3.5	36.4	0.0
(b) Pt-Impregnated Catalysts							
After 5 min							
Pt/SZ	38.3	92.6	0.0	0.8	2.1	35.4	0.0
Pt/SAZ*i*-3	36.5	94.2	0.0	0.9	1.3	34.3	0.0
Pt/SGZ*i*-3	48.2	88.9	0.0	1.7	3.7	42.8	0.0
Pt/SAZ*c*-3	46.5	88.8	0.0	1.8	3.5	41.3	0.0
Pt/SGZ*c*-3	59.5	72.9	1.9	3.4	10.8	43.4	0.0
Steady regime							
Pt/SZ	30.2	95.6	0.0	0.0	1.3	28.9	0.0
Pt/SAZ*i*-3	30.9	95.8	0.0	0.3	1.0	29.6	0.0
Pt/SGZ*i*-3	37.5	92.5	0.0	1.1	1.7	34.7	0.0
Pt/SAZ*c*-3	38.1	92.5	0.0	1.1	1.8	35.2	0.0
Pt/SGZ*c*-3	51.7	83.0	0.9	2.2	5.7	42.9	0.0

DISCUSSION

The main features emerging from the catalytic results may be summarized as follows: (i) promotion with Al or Ga, whether by impregnation or coprecipitation, enhanced the catalytic properties and stability relative to pure sulfated zirconia, confirming reported results over SAZ catalysts (e.g., 8, 39, 40); (ii) the promoted catalysts prepared by

coprecipitation were more efficient than those obtained by impregnation, with the Ga coprecipitated catalyst being superior to the Al analogue; and (iii) platinum deposition increased the catalytic performances with respect to the Pt-free forms.

The principal parameters which distinguish the catalysts obtained with the two preparation methods are surface area, monoclinic/tetragonal fraction, amount of sulfate, acid content, and nature of the promoter. In the literature, the catalytic results over nonpromoted and promoted sulfated zirconias have been discussed in terms of crystalline phase(s), sulfate content (surface densities, coverage), and acidity (the nature of which is influenced by the presence of water).

The SZ catalyst contained a substantially higher fraction of monoclinic structure than the promoted ones, with this phase being more developed in the catalysts obtained by impregnation than by coprecipitation, and almost absent in the most active SGZ*c*-3 catalyst. Promotion with Al and Ga stabilized the tetragonal phase, independent of the presence or absence of sulfate. Indeed, the XRD patterns of both the coprecipitated mixed oxides and those prepared by impregnation calcined at 650°C (no sulfate) showed exclusively the reflections of the tetragonal phase. In contrast, pure zirconia was totally monoclinic. A similar effect has been observed with other promoters, e.g., Y_2O_3 (41). It has been shown that the sulfated monoclinic structure was poorly efficient in *n*-butane isomerization (42, 43), and inactive in hexane isomerization (44). This would account for the lower conversions observed for SZ. Attempts to prepare SZ catalysts with higher amounts of sulfate failed. After calcination at 650°C, sulfate contents of 4.14, 4.37, 4.37, and 4.50% were found for nominal weight percentages of sulfate introduced at the impregnation step of 5, 7.5, 10, and 15%, respectively (sulfate densities between 2.5 and 3.1 SO_4^{2-} nm^{-2}). The fractions of monoclinic structure were around 28–30%, and the conversion–time curves nearly superimposed, with steady conversion of about 20–23%. This suggests that without promoter, the amount of sulfate that can be retained on the solid calcined at 650°C remained insufficient to prevent the formation of the monoclinic structure. As illustrated in Fig. 7, the conversions after 5 min decreased proportionally to the fraction of monoclinic phase in the catalysts, with a conversion of about 7% for a SZ sample with 80% monoclinic structure (2.44% sulfate, 53% coverage), whereas a negative exponential-type curve was obtained with the values at steady conversion, indicating that other factors also have to be considered, principally, as discussed below, the loss of the very strong acid sites in the early stage of the reaction.

Gao *et al.* (8) and Xia *et al.* (39) proposed that Al incorporation (with a higher electronegativity than Zr) in the ZrO_2 matrix brought about an increase of the positive partial charge on the Zr cations as a result of the formation of Zr–O–Al bonds which helped to stabilize the sulfate

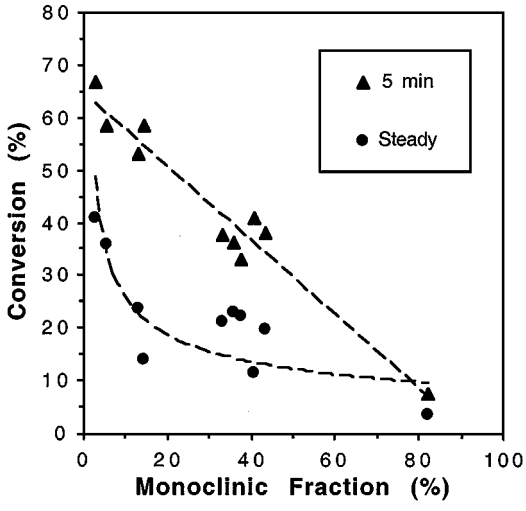

FIG. 7. Relation between initial and steady conversion vs fraction of monoclinic structure.

species at the oxide surface (with an increase of the number of strong acid sites). In this study, the XPS data showing such bonds in SAZ*c* and SGZ*c* (much less so for the SMZ*i* catalysts), and the sulfate densities increasing in the order SZ < SMZ*i* < SMZ*c* are apparently consistent with that proposal. The similar sequence of tetragonal fraction and sulfate densities of the different catalysts suggests that both are inter-related, with the promoter effect on sulfate retention being merely due to the stabilization effect it has on the tetragonal structure. The sulfate content of SZ and the catalysts prepared by impregnation, with higher fractions of monoclinic phase, was insufficient to ensure a complete monolayer (namely, 4 SO_4^{2-} nm^{-2}), whereas monolayer coverage was achieved for SGZ*c*-3, nearly exempt of this structure. SAZ*c*-3, with an excess of sulfate with respect to monolayer coverage, contained a little more monoclinic phase. It has been shown that overlayer sulfates decreased the stabilization of the tetragonal phase (45), and hindered the isomerization activity (46), which is in line with our results. The importance of surface coverage on the catalytic efficiency of sulfated zirconias was also stressed by Laizet *et al.* (44) and, in agreement with those authors, it may be concluded that this factor is primordial to the catalytic activity of these materials. The cited authors related the essential role of the tetragonal phase to the higher number of Zr coordinative bonds (weaker Zr–O bond strength) which, upon activation, should facilitate the formation of Zr^{3+} Lewis sites and nearby Brønsted SO–H sites. Both our characterization results and catalytic data are partly consistent with this observation.

With respect to the relation surface coverage–acidity–activity, it is not clear from the literature which type of acid sites are active in butane isomerization over SZ catalysts. One reason for this situation is that the acidity determinations have often been carried out under conditions quite

different from those prevailing for the catalytic measurements, which may have a dramatic importance for catalysts as sensitive to water as sulfated zirconias. Some authors proposed that only Lewis acidity would be involved (3, 22, 47–50). Other authors (51, 52) found a relationship between the activity and the B/L ratio, a catalyst with only L sites being inactive. For Yaluris *et al.* (53), the intervention of B sites (largely overwhelming the L acidity) would predominate, as clearly demonstrated by selective poisoning experiments with ammonia, with the L sites possibly contributing to a reinforcement of the strength of the B sites via inductive effects, as also proposed by Laizet *et al.* (44). Zalewski *et al.* (54) observed, in isobutane/2-butene alkylation over a sulfated ZrO_2 stabilized with 20 wt% alumina, that the number of Brønsted acid sites reached a maximum for a sulfate loading, ensuring near monolayer coverage. Gao *et al.* (8) attributed the long-term activity of their most active SAZ catalyst (3% Al_2O_3, 86% coverage) relative to SZ to the higher amount of acid sites with differential heat of ammonia adsorption between 125 and 140 kJ mol^{-1}. Yaluris *et al.* (53) found similar values for the acid sites responsible for the long-term activity ("standard activity") of SZ catalysts. In contrast, other authors observed a maximum of activity for a SAZ catalyst with sulfate content corresponding to 3.5 SO_4^{2-} nm^{-2} (87.5% of a sulfate monolayer), without appreciable difference of the Lewis and Brønsted acidity with respect to sulfated zirconia (23, 55). However, using a new approach for the determination of the Brønsted acid sites, Olindo *et al.* (56) recently reported that a SAZ catalyst with 2.7 mol% Al_2O_3 contained twice as many Brønsted sites as nonpromoted sulfated zirconia. Note that in the studies cited above, the maximum activity occurring for a surface coverage near to monolayer is probably not fortuitous.

In this work, the higher intensity of the OH band at 3560–3570 cm^{-1}, the greater amounts of adsorbed ammonia, and the higher content and strength of the B acid sites of the promoted catalysts relative to pure sulfated zirconia are in line with both the higher (initial) activity of the former catalysts and literature results (8, 56). However, the higher steady conversion achieved over the coprecipitated catalysts compared to those obtained by impregnation (Table 3a) can hardly be accounted for by differences in acid contents alone (Table 1) suggesting, in agreement with other authors (28), that strong acidity is necessary but not sufficient to account for the higher activity of the coprecipitated catalysts and, as stressed earlier, differences of surface coverage by sulfate species and fraction of the tetragonal structure also need to be taken into account. As shown in Fig. 6a and Table 3, the high initial conversion followed by steep decrease in the first hour of reaction over the Pt-free catalysts, mainly due to a rapid diminution of propane in the first 30 min of reaction, and also of C2 and i-C5 for the Al- and Ga-modified zirconias, seems to involve very strong acid sites which are rapidly lost. A similar result was related by Gao *et al.* (8) to strong acid sites with differential heat of ammonia adsorption above 140 kJ mol^{-1}. For Yaluris *et al.* (53), the strong acidity would predominantly involve Brønsted sites (with heat of ammonia adsorption between 145 and 165 kJ mol^{-1}), possibly associated with L sites accounting for the "excess" (initial) activity. Recently, Katada *et al.* (57) showed that the most active sulfated zirconias for butane isomerization (with coverage by sulfate of about 90%, and differential adsorption enthalpies of ammonia of 160 kJ mol^{-1}) contained both Brønsted and Lewis acidities, in a B/B + L ratio of about 0.2 (estimated from the intensity of the characteristic IR bands of adsorbed pyridine, at 1545 cm^{-1} for Py-B, and 1455 cm^{-1} for Py-L). For those authors, the simultaneous presence of B and L sites would enhance the catalytic activity, possibly via a concerted action of paired B and L sites, as proposed by Clearfield *et al.* (58). (Note that a similar concerted effect or synergism between B and L sites has also been advocated to account for enhanced activities of zeolites.). This result appears in contradiction with the overwhelming presence of Brønsted sites as observed in this study by IR spectroscopy of adsorbed ammonia. The different pretreatment conditions adopted by the cited authors and possible overestimation of the Lewis acidity by pyridine measurement, as recently shown by Morterra *et al.* (59), may account for the misfit between our results and those of Katada *et al.* (57). So far, it is not clear whether the promoters contribute directly to the strong acidity or only indirectly by favoring both the tetragonal structure and sulfate retention. Olindo *et al.* (23) found that water was more difficult to remove from Al-promoted catalysts compared with sulfated zirconia, an observation also made in this study. It could be speculated that in highly dehydrated samples some residual water molecules strongly polarized on coordinatively unsaturated Al and Ga ions could undergo partial dissociation, giving M–OH-type species and protons. Those extra protons could form additional H_3O^+ groups (accounting for the higher B acid contents and the higher intensity of the OH band at 3560 cm^{-1}), and bisulfate species proposed by several authors as the active species (e.g., 30, 58, 60). The higher electronegativity of Ga vs Al would favor the former one.

Skeletal isomerization of *n*-butane over SZ and Pt/SZ catalysts may occur, according to the authors, mainly via an intramolecular (e.g., 61, 62) or bimolecular mechanism. Recent kinetic results over Pt/SZ catalysts favored the second mechanism in which butenes (as impurity in the feed or produced by dehydrogenation) react with a butyl carbenium to form an i-$C8^+$ intermediate, followed by skeletal isomerization (hydride and methyl shift) and scission in a butyl carbenium and i-C4 (63). A bimolecular mechanism was recently confirmed from experiments with ^{13}C-labelled *n*-butane over SZ catalyst (64). In parallel, cleavage of i-C8 in equal amounts of C3 and i-C5 may also occur. It has also been proposed that both mono- and bimolecular mechanisms may compete, the one prevailing over the other

one depending on the reaction conditions (presence of a diluent gas, reaction temperature, etc.) (65–67).

The results obtained in this study (without and with platinum) merely suggest a bimolecular pathway. The presence of i-C5 among the reaction products for the Pt-free catalysts implies a scission of part of the C8 intermediates at the early stage of the reaction, namely, where the very strong acid sites operate. The greater abundance of C3 over i-C5 (with the latter being detected only within the first 5–30 min of reaction) suggests that the reaction is probably more complex, since simple cleavage of i-C8 intermediate should produce equal amounts of C3 and i-C5 throughout the reaction. Further cracking of i-C5 in C2 and C3 cannot be excluded although the C3/C2 ratio should be 2. Some authors suggested that the increasing amounts of light products (C1–C3) could be due to a cracking of butane (63), while other authors suggested that C5 products could react with an adsorbed carbenium ion to form C9 which, in turn, could isomerize and crack in C3 and C6 (53), with further cleavage of C6 in 2C3 (68). In this study, C6 was not identified among the reaction products and the absence of methane allows one to rule out a simple cracking of butane in C1 and C3. Although the monomolecular mechanism cannot be rejected, the results suggest that i-C4 is mainly formed via an oligomerization–isomerization–cracking pathway.

Platinum deposition decreased the initial conversion especially for the promoted catalysts. It also decreased the deactivation rate of all catalysts, resulting in improved long-term conversion (Fig. 6b and Table 3). These observations are consistent with results reported over sulfated zirconias (e.g., 6, 63, 69, 70). The improvement was relatively more important for the nonpromoted Pt/SZ catalyst with a conversion 2.6 times higer relative to that for SZ after 10 h on stream. Addition of platinum transforms an essentially acidic catalyst to a bifunctional one, where the metal function operates butane dehydrogenation–hydrogenation. According to Liu *et al.* (63), the butene consumed in a bimolecular mechanism would be continuously regenerated by the presence of Pt with, as a result, higher conversion and increased stability. The lower initial conversions of the promoted catalysts seem to indicate that the very strong acid sites responsible for the high initial values over the platinum-free catalysts were less abundant (perhaps absent) in the Pt-loaded samples. Among possible causes which can be suggested, it may well be that the water produced by the reduction of platinum at 250°C (estimated at 15 or 30 μmol g^{-1}, according to the oxidation state of the metal) is probably mostly retained on the strongly hygroscopic sulfate groups of the promoted catalysts and could thus modify the nature (and/or strength) of the active sites. As mentioned earlier, water was more difficult to remove from promoted catalysts than from SZ, and as seen in Table 1, the water content of the catalysts was directly related to the amount of sulfate. Alternatively, Liu *et al.* (63) showed that the initial isomerization rate and the deactivation rate significantly decreased when the concentration of butene in the feed was reduced. Accordingly, in the presence of Pt, the lower initial conversions could be the result of the rapid hydrogenation of butene impurities in the feed. For the Ga-containing catalysts, Pt addition also suppressed the particular behavior noticed over the Pt-free form for a reason which still has to be clarified. Perhaps addition of platinum would favor partial *in situ* reduction of Ga^{3+} to Ga^{+} by spillover hydrogen on the metal particles (71), hence reinforcing the dehydrogenation function and the formation rate of the intermediates, although no experimental evidence supporting this assumption can presently be provided.

CONCLUSIONS

Promotion of sulfated zirconia with Al and Ga (3 mol% as oxide) improved the efficiency and stability of sulfated zirconias in *n*-butane isomerization, with a more substantial effect when the promoter was introduced via coprecipitation rather than by impregnation. Promotion enhanced the stability of the tetragonal structure and the sulfate retention of the solids with, as a result, an increase of strong Brønsted acid sites content with respect to nonpromoted sulfated zirconia. Fractions of tetragonal structure and sulfate densities (or coverage) were found to play an essential role in the catalysts activity. Strong acidity was necessary but not a main condition. Ga was a more efficient promoter than Al when introduced via coprecipitation. The best catalytic performances were obtained over sulfated Ga-promoted zirconia nearly free of monoclinic structure and with nearly monolayer sulfate coverage. Ga-promoted catalysts exhibited a particular behavior in the course of the reaction for a reason which is not fully clarified. In the absence of platinum, the high conversion levels in the first period of the reaction followed by a steep decrease suggested the intervention of very strong acid sites which were rapidly lost. Platinum addition significantly increased the overall *n*-butane conversion of all catalysts, at some expense of the selectivity to i-C4 due to enhanced hydrogenolysis–cracking reactions. The presence of Pt also suppressed the steep activity loss of the Ga-promoted catalysts.

ACKNOWLEDGMENTS

J.A.M. gratefully acknowledges Colciencias, Colombia, for financial support. This research was partly carried out in the frame of E.U. "Hydroconv" Network.

REFERENCES

1. Frischkorn, G. L., Kuchar, P. J., and Olson, R. K., *Energy Prog.* **8**, 159 (1988).
2. Arata, K., *Adv. Catal.* **37**, 165 (1990).

3. Tanabe, K., Hattori, H., and Yamaguchi, T., *Crit. Rev. Surf. Chem.* **1**, 1 (1990).
4. Hsu, C. Y., Heimbuch, C. R., Armes, C. T., and Gates, B. C., *J. Chem. Soc., Chem. Commun.* 1645 (1992).
5. Song, X., and Sayari, A., *Catal. Rev. Sci. Eng.* **38**(3), 329 (1996).
6. Baba, S., Shibata, Y., Kawamura, T., Takaoka, H., Kimura, T., Kousaka, K., Minato, Y., Yokoyama, N., Lida, K., and Imai, T., Eur. Patent 174836, 1985.
7. Marella, M., Tomaselli, M., Meregalli, L., and Pinna, F., Eur. Patent 983967, 2000.
8. Gao, Z., Xia, Y., Hua, W., and Miao, C., *Topics Catal.* **6**, 101 (1998).
9. Lei, T., Xu, J. S., Hua, W. M., Tang, Y., and Gao, Z., *Catal. Lett.* **61**, 213 (1999).
10. Lei, T., Xu, J. S., Tang, Y., Hua, W. M., and Gao, Z., *Appl. Catal. A: Gen.* **192**, 181 (2000).
11. Angelescu, E., Ropot, M., Contantinescu, F., Boiangiu, D., and Pencea, M., *Prog. Catal.* **7**, 5 (1998).
12. Zhao, E., Isaev, Y., Skyarov, A., and Fripiat, J. J., *Catal. Lett.* **60**, 173 (1999).
13. Toraya, H., Yoshimura, M., and Somiya, S., *J. Am. Ceram. Soc.* **67**, C-119 (1984).
14. Moreno, J. A., and Poncelet, G., *Appl. Catal. A: Gen.* **210**, 151 (2001).
15. Sing, K. S. W., and Rouquerol, J., *in* "Handbook of Heterogeneous Catalysis" (G. Ertl, H. Knözinger, and J. Weitkamp, Eds.), Vol. 2, p. 427. Wiley-VCH, Berlin, 1997.
16. Chen, F. R., Coudurier, G., Joly, J. F., and Vedrine, J. C., *J. Catal.* **143**, 616 (1993).
17. Hua, W., Xia, Y., Yue, Y., and Gao, Z., *J. Catal.* **196**, 104 (2000).
18. Phillipi, C. M., and Mazdiyasni, K. S., *J. Am. Ceram. Soc.* **54**, 254 1 (971).
19. Riemer, T., Spielbauer, D., Hunger, M., Mekhemer, G. A. H., and Knözinger, H., *J. Chem. Soc., Chem. Commun.* 1181 (1994).
20. Barthos, R., Lonyi, F., Onuestyak, G., and Valyon, J., *J. Phys Chem.* **104**, 7311 (2000).
21. Gorte, R. J., *Catal. Lett.* **62**, 1 (1999).
22. Morterra, C., Cerrato, G., Pinna, F., Signoretto, M., and Strukul, G., *J. Catal.* **149**, 181 (1994).
23. Olindo, R., Pinna, F., Strukul, G., Canton, P., Riello, P. Cerrato, G., Meligrana, G., and Morterra, C., *in* " Proc., 12th International Congress on Catalysis, Granada, Spain, 2000" (A. Corma, F. V. Melo, S. Mendioroz, and J. L. G. Fierro, Eds.), Studies in Surface Science and Catalysis, Vol. 130, p. 2375. Elsevier, Amsterdam, 2000.
24. Morterra, C., Cerrato, A., Pinna, F., and Signoretto, M., *J. Catal.* **157**, 109 (1995).
25. Babou, F., Coudurier, G., and Vedrine, J. C., *J. Catal.* **152**, 341 (1995).
26. Kustov, L. M., Kazansky, V. B., Figueras, F., and Tichit, D., *J. Catal.* **150**, 143 (1994).
27. Little, L. H., "Infrared Spectra of Adsorbed Species," p. 230. Academic Press, New York, 1966.
28. Gonzalez, M. R., Kobe, J. M., Fogash, K. B., and Dumesic J. A., *J. Catal.* **160**, 290 (1996).
29. Morterra, C., Cerrato, G., Di Ciero, S., Signoretto, M., Pinna, F., and Strukul, G., *J. Catal.* **165**, 172 (1997).
30. Morterra, C., Cerrato, G., Pinna, F., and Signoretto, M., *J. Phys. Chem.* **98**, 12373 (1994).
31. Teunissen, E. H., van Santen, R. A., Jansen, P. J., and van Duijneveldt, F. B., *J. Phys. Chem.* **97**, 203 (1993).
32. Tsyganenko, A. A., Pozdnyakov, D. V., and Filimonov, V. N., *J. Mol. Struct.* **29**, 299 (1975).
33. Topsoe, N.-Y., Dumesic, J. A., and Topsoe, H., *J. Catal.* **151**, 241 (1995).
34. Ramis, G., Busca, G., Bregani, F., and Forzatti, P., *Appl. Catal.* **64**, 259 (1990).
35. Zecchina, A., Marchese, L., Bordiga, S., Pazè, C., and Gianotti, E., *J. Phys. Chem. B* **101**, 10128 (1997).
36. Spielbauer, D., Mekhemer, G. A. H., Zaki, M. I., and Knözinger, H., *Catal. Lett.* **40**, 71 (1996).
37. Bensitel, M., Saur, O. Lavalley, J. C., and Morrow, B. A., *Mater. Chem. Phys.* **19**, 147 (1998).
38. Haase, F., and Sauer, J., *J. Am. Chem. Soc.* **120**, 13503 (1998).
39. Xia, Y., Hua, W., and Gao, Z., *Appl. Catal. A: Gen.* **185**, 293 (1999).
40. Hua, W., Goeppert, A., and Sommer, J., *J. Catal.* **197**, 406 (2001).
41. Morinaga, M., Cohen, J. B., and Faber, J., *Acta Crystallogr. A* **35**, 789 (1979).
42. White, R. L., Sikabwe, E. C., Coelho, M. A., and Resasco, P. E., *J. Catal.* **157**, 755 (1995).
43. Stichert, W., and Schüth, F., *J. Catal.* **174**, 242 (1998).
44. Laizet, J. B., Soiland, A. K., Leglise, J., and Duchet, J. C., *Topics Catal.* **10**, 89 (2000).
45. Farcasiu, D., Li, J. Q., and Cameron, S., *Appl. Catal. A: Gen.* **154**, 173 (1997).
46. Bedilo, A. F., and Klabunder, K. J., *J. Catal.* **176**, 448 (1998).
47. Yamaguchi, T., *Appl. Catal.* **61**, 1 (1990).
48. Yamaguchi, T., Jin, T., and Tanabe, K., *J. Phys. Chem.* **90**, 3148 (1986).
49. Yamaguchi, T., Jin, T., Ishida, T., and Tanabe, K., *Mater. Chem. Phys.* **17**, 3 (1987).
50. Pinna, F., Signoretto, M., Strukul, G., Cerrato, G., and Morterra, C., *Catal. Lett.* **26**, 339 (1994).
51. Nascimento, P., Akratopoulou, C., Oszagyan, M., Coudurier, G., Travers, C., Joly, J. F., and Vedrine, J. C., *in* "New Frontiers in Catalysis" (L. Guczi, Ed.), p. 1186. Elsevier, Amsterdam, 1992.
52. Ward, D. A., and Ko, E. I., *J. Catal.* **150**, 18 (1994).
53. Yaluris, G., Larson, R. B., Kobe, J. M. Gonzalez, M. R., Fogash, K. B., and Dumesic, J. A., *J. Catal.* **158**, 336 (1996).
54. Zalewski, D. J., Alerasool, S., and Doolin, P. K., *Catal. Today* **53**, 419 (1999).
55. Pinna, F., Olindo, R., Strukul, G., Cerrato, G., and Morterra, C., "4th European Congress on Catalysis (Europacat), Rimini," Book of Abstracts, p. 719. Italy, 1999.
56. Olindo, R., Goeppert, A., Habermacher, D., Sommer, J., and Pinna, F., *J. Catal.* **197**, 344 (2001).
57. Katada, N., Endo, J., Notsu, K., Yasunobu, N., Naito, N., and Niwa, M., *J. Phys. Chem. B* **104**, 10321 (2000).
58. Clearfield, A., Serrette, G. P. D., and Khazi-Syed, A. H., *Catal. Today*, **20**, 295 (1994).
59. Morterra, C., Cerrato, G., Pinna, F., and Meligrana, G., *Topics Catal.* **15**, 53 (2001).
60. Saur, O., Bensitel, M., Saad, A. B. M., Lavalley, J. C., Tripp, C. P., and Morrow, B. A., *J. Catal.* **99**, 104 (1984).
61. Garin, F., Andriamasinoro, D., Abdulsamad, A., and Sommer, J., *J. Catal.* **131**, 199 (1991).
62. Tomishige, K., Okabe, A., and Fujimoto, K., *Appl. Catal. A: Gen.* **194–195**, 383 (2000).
63. Liu, H., Adeeva, V., Lei, G. D., and Sachtler, W. M. H., *J. Mol. Catal.* **100**, 35 (1995).
64. Kim, S. Y., Goodwin, Jr., J. G., and Farcasiu, D., *Appl. Catal. A: Gen.* **207**, 281 (2001).
65. Tran, M.-T., Gnep, N. S., Guisnet, M., and Nascimiento, P., *Catal. Lett.* **47**, 57 (1997).
66. Matsuhashi, H., Shibata, H., Nakamura, H., and Arata, K., *Appl. Catal. A: Gen.* **187**, 99 (1999).
67. Suzuki, T., and Okuhara, T., *Chem. Lett.* 470 (2000).
68. Tran, M.-T., Gnep, M. S., Szabo, G., and Guisnet, M., *Appl. Catal. A: Gen.* **171**, 207 (1998).
69. Hosoi, T., Shimidsu, T., Itoh, S., Baba, S., Takahoka, H., Imai, T., and Yokoyama, N., "Proc. ACS, Los Angeles Meeting 1988," p. 562. Am. Chem Soc., Washington, DC., 1988.
70. Garin, F., Seyfried, L., Girard, P., Maire, G., Abdulsamad, A., and Sommer, J., *J. Catal.* **151**, 26 (1995).
71. Shpiro, E. S., Shevchenko, D. P., Dmitriev, R. V., Tkachenko, O. P., and Minachev, Kh. M., "Studies in Surface Science and Catalysis," Vol. 77, p. 159. Elsevier, Amsterdam, 1993.